Connection between giant magnetoresistance and structure in molecular-beam epitaxy and sputtered Fe/Cr superlattices

José M. Colino and Ivan K. Schuller

Department of Physics 0319, University of California-San Diego, La Jolla, California 92093

R. Schad,* C. D. Potter,† P. Beliën,‡ G. Verbanck, V. V. Moshchalkov, and Y. Bruynseraede

Laboratorium Voor Vaste-Stoffysika en Magnetisme, Katholieke Universiteit Leuven, Leuven, Belgium, B 3001

(Received 22 June 1995; revised manuscript received 7 September 1995)

We have performed a comparison of magnetoresistance and structure of epitaxial and textured Fe/Cr super-lattices grown by molecular-beam epitaxy (MBE) and magnetron sputtering with either (110) and (100) orientations on a variety of substrates. MBE samples grown along the (100) orientation, exhibit narrower rocking curves (mosaic spread) and lower saturation resistivities than sputtered samples. On the other hand, (110) MBE and sputtered samples have comparable saturation resistivities. The magnetoresistance ($\Delta\rho$) of MBE and sputtered samples are comparable. Epitaxial MBE samples, with small rocking curves, show a clear correlation between the magnetoresistance and rocking curve width. In sputtered samples, roughness, controlled by the deposition pressure, plays an important role although the general trends depend on orientation and mosaic spread of the samples.

INTRODUCTION

Since the discovery of giant magnetoresistance (GMR) in Fe/Cr superlattices[1] many groups have investigated the details of this interesting phenomenon[1-6] although the actual values of GMR ($\Delta\rho/\rho_s$; $\Delta\rho=\rho[H=0]-\rho_s$) are scattered from lab to lab and depend on deposition method, substrate, crystalline orientation, texture, interface properties, etc. GMR's range typically from 1–2 % in trilayers[7] up to $\sim$220% in molecular-beam epitaxy (MBE) grown (100) [Fe(5 Å)/Cr(12 Å)]$_{50}$.[5] Also, their structural properties strongly depend on the growth method, substrate, crystallographic orientation, number of bilayers, growth temperature, thickness of each element, etc. Clearly, structural parameters control the value of $\Delta\rho/\rho$ and it is therefore desirable to perform controlled experiments in which the effect of structure on the GMR is investigated. We have performed a detailed magnetotransport and structural study of Fe/Cr super-lattices grown by MBE and sputtering as a function of crystalline orientation, roughness, and texture. Several general common trends are observed, such as systematic changes of saturation resistivity (ρ_s) and magnetoresistance ($\Delta\rho$) with the mosaicity in (100) samples. Other properties drastically change with growth conditions and do not exhibit a general trend. These data show that GMR phenomena are controlled in subtle ways by structural parameters and therefore detailed structural studies must play a crucial role in all these studies.

EXPERIMENTAL

Sputtered superlattices of [Fe(30 Å)/Cr(t)]$_{10}$(110) were directly grown on room temperature Si wafers[4] and [Fe(30 Å)/Cr(t)]$_{10}$(100) on single crystal MgO(100) substrates at $\sim$180 °C. Fe/Cr superlattices were prepared by MBE at a rate of 1 Å/s with or without a 50 Å Cr seed layer on MgO(100), MgO(110), GaAs(110), GaAs(100), and SrF$_2$(111) substrates. Further deposition details have been published elsewhere.[4,5] Structural characterization was performed *ex situ* using high- and low-angle x-ray diffraction on a Rigaku rotating anode x-ray diffractometer with Cu-K_α radiation. The magnetization was obtained from superconducting quantum interference device (SQUID) magnetometry at 10 K. Four lead magnetotransport measurements were performed at liquid helium temperatures and magnetic fields well-above saturation on as-grown (Van der Pauw method) or lithographically patterned samples. The magnetic field was in the film plane and perpendicular to the dc electrical current.

RESULTS AND DISCUSSION

Figure 1(a) shows the saturation resistivity of (100) Fe/Cr superlattice sputtered at different pressures and grown by MBE with and without Cr seed layer as a function of (200) rocking curve width ($\Delta\varphi$). Despite the variation of Cr thicknesses and other above-mentioned growth parameters, ρ_s follows a clear trend increasing with $\Delta\varphi$ for all the samples. This implies that grain boundary scattering is an important mechanism contributing to the resistivity for all the (100) samples. Single (100) layers of Fe and Cr of thickness 20–1100 Å prepared under identical condition by MBE have lower bulk resistivities (0.2–0.35 $\mu\Omega$ cm) (Ref. 5) than the resistivity of the superlattice extrapolated to $\Delta\varphi=0$ ($\sim$8 $\mu\Omega$ cm). This implies that about $\sim$8 $\mu\Omega$ cm is due to interface scattering, since $\Delta\varphi=0$ implies the probable absence to grain boundaries. Other authors have reported single-layer resistivities comparable to the superlattice values for sputtered epitaxial samples.[6] Figure 1(b) shows the dependence of the saturation resistivity on rocking curve width $\Delta\varphi$ for the (110) samples. Note that in this case the resistivity is independent of $\Delta\varphi$, $\rho_s=24\pm5$ $\mu\Omega$ cm. These facts suggest that for the (110) samples grain boundary scattering plays a lesser role in the (100) samples. However, Fig. 1(b) shows
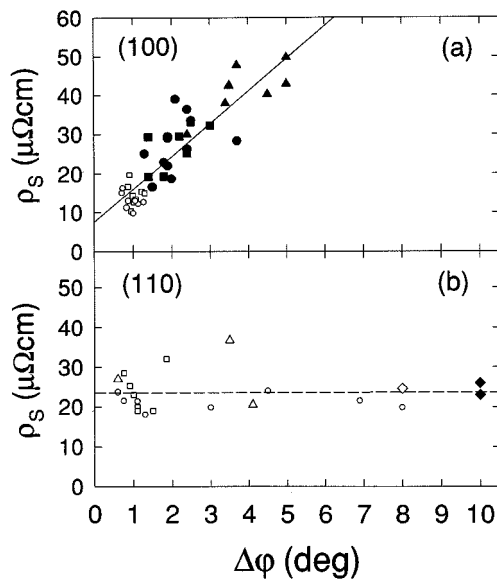
FIG. 1. (a) Saturation resistivity versus the rocking curve width (FWHM) of all (100) Fe/Cr multilayers on MgO(100) substrates grown under different conditions; (□) by MBE without a Cr seed layer, (○) by MBE with a 20 Å Cr seed layer, (●) by sputtering at an argon pressure of 4 mTorr, (■) by sputtering at 7 mTorr, and (▲) by sputtering at 11 mTorr. The straight line is a least-squares fit. (b) Saturation resistivity versus rocking curve width for all (110) samples on different substrates; (◆) sputtered on Si, (△) MBE on GaAs, (◇) MBE on SrF$_2$, (○) MBE on MgO(110) with a Cr seed, and (□) MBE on MgO(110) without a Cr seed. Dashed line is a least-squares fit.

FIG. 2. (a) Magnetoresistance as a function of the high-angle rocking curve width for all (100) samples at the first AF peak (Cr =13–15 Å); (□) by MBE without a Cr seed layer, (○) by MBE with a 50 Å Cr seed layer, (●) by sputtering at an argon pressure of 4 mTorr, (■) by sputtering at 7 mTorr and (▲) by sputtering at 11 mTorr. The lines are least-squares fits. (b) Same magnitudes for all the (110) Fe/Cr samples; (◆) sputtered on Si, (△) MBE on GaAs, (◇) MBE on SrF$_2$, (○) MBE on MgO(110) with a Cr seed, and (□) MBE on MgO(110) without a Cr seed.

greater resistivities of epitaxial MBE (110) samples than the MBE (100) samples for *mosaic spread widths* ($\Delta\varphi$) below ~1°. These differences between the (100) and (110) samples suggest an influence on the resistivity of the crystalline orientation perhaps through the electronic structure[11] and/or differences in growth mechanism due to changes in surface diffusion with orientation. In fact, (100) Fe/Cr growth seems to be epitaxially driven on MgO(100), especially with a Cr seed layer, whereas (110) Fe/Cr on a variety of strongly mismatched substrates is a result of surface energy minimization on closed packed planes. These differences could account for different roles of the mosaic spread in the leading scattering mechanism.

Figure 2(a) is a plot of the magnetoresistance ($\Delta\rho$) as a function of the mosaic spread ($\Delta\varphi$) for all the (100) samples grown with Cr thicknesses at the first antiferro (AF) peak. Only these are shown because $\Delta\rho$ depends strongly, i.e., oscillates, with the Cr thickness.[3] The rocking curve widths vary with substrate, seed layer, deposition rates or perhaps some uncontrolled deposition parameters. While the sputtered samples exhibit a constant magnetoresistance for every deposition pressure, the epitaxial and textured MBE samples show a rapid variation for the samples with small $\Delta\varphi$. It should be stressed that the highest magnetoresistance of the MBE (12–13 $\mu\Omega$ cm) and "4-mTorr" sputtered samples (~8–9 $\mu\Omega$ cm) are comparable. Therefore the considerably higher GMR, $\Delta\rho/\rho$, in MBE samples is mostly due to smaller resistivities, e.g., spin-independent scattering. Figure 2(b) shows an overall lower $\Delta\rho$ for both epitaxial and textured (110) samples compared to that of (100) superlattices. Again,
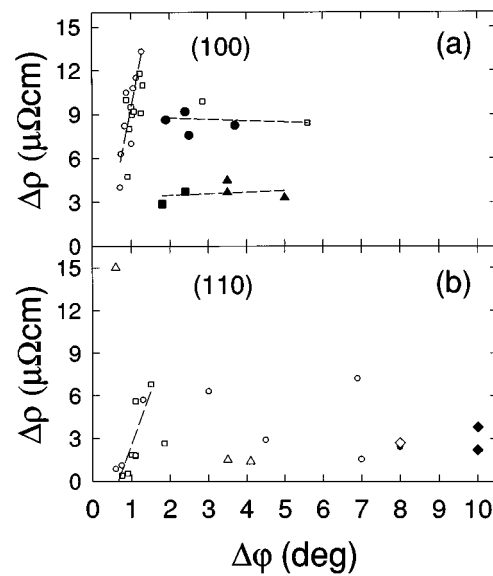
the magnetoresistance of epitaxial MBE samples varies rapidly at low $\Delta\varphi$ (dashed line). An inspection of Fig. 2 shows that, certainly for the (100) and perhaps for the (110) orientation, there is an optimum value of the rocking curve width (~1.2–1.6°) which maximizes the magnetoresistance. This implies therefore that there are two competing mechanisms contributing to the magnetoresistance: interfacial scattering which increases the magnetoresistance and grain boundary scattering which decreases it because it reduces the contribution from the interface. For small $\Delta\varphi$, a large fraction of the resistivity comes from interfacial scattering. Increasing $\Delta\varphi$ increases the interfacial faceting thereby enhancing $\Delta\rho$. At large values of $\Delta\varphi$, the strong grain boundary scattering dominates the scattering and makes the magnetoresistance constant. A larger GMR with increased grain size has been found by Modak, Smith, and Parkin[8] from transmission electron microscopy investigations in two epitaxial Co/Cu samples, and attributed it to an increased mean free path leading to a sampling of more antiferromagnetically coupled layers. The existence of an optimum roughness for maximum GMR was already suggested by Petroff *et al.*[9]

An important issue is the role of the crystallographic orientation on the absolute value of GMR. Recently Parkin, Rabedeau, and Modak[10] reported identical value at the first GMR peak for Co/Cu multilayers with three different orientations: (100), (110), and (111). Fullerton *et al.*,[11] on the other hand, found significant differences between the magnetoresistance of (100) and (211) Fe/Cr samples with similar resistivities and mosaic spread. The present data for Fe/Cr, Fig. 2, shows consistently an overall greater $\Delta\rho$ for (100) than (110) samples, which implies that Fermi surface nesting of the Cr spacer plays an important role on the GMR value.

Finally an important open issue is the influence of the interfacial roughness on the giant magnetoresistance. It is known that the bulk and/or interface structure of sputtered multilayers can be altered by varying the deposition pressure. Fullerton *et al.* showed an increase on the interfacial roughness of (110) sputtered [Fe(30 Å)/Cr(18 Å)]$_{10}$ with an increasing Ar pressure and achieved an increased GMR, from 6% to ~13% in the rougher samples.[4] This is consistent with earlier measurements by Petroff *et al.*[9] Rensing, Payne, and Clemens made a similar study in (110) Fe(30 Å)/Cr(*t*) trilayers as a function of Cr thickness and did not observe such an increased GMR with roughness at the first AF peak, rather for Cr thicknesses between the first and second peaks.[12] It should be pointed out that in this latter case, the structural and magnetotransport measurements were performed on different sets of samples. Nevertheless, in both cases it was found that for multilayers the interface becomes more disordered with increasing sputtering pressure. This manifests itself as increased superlattice linewidths and disappearance of finite size peaks in the low angle x-ray spectra,[13] as shown in Fig. 3(b) for Fe/Cr samples grown on Si or sapphire substrates.

Figure 3 shows the low angle x-ray diffraction from (100) samples (a) and (110) samples (b) grown by sputtering at different argon pressures. Qualitatively, the presence of low angle peaks up to 7°–8° is an indication of smooth layered growth and can be used to determine the average thickness of the layers. Moreover, these plots indicate a higher degree of short-range roughness in the (110) samples. Unfortunately, a quantitative analysis[14] of the interface structure is hampered by the low contrast in electron density between Fe and Cr. Similar results are obtained for the best samples with either growth method. However, the correlation of low-angle specular data with transport properties is complicated by the dependence on other structural parameters. Large, qualitative changes may be induced in these spectra by varying the sputtering pressure.

To investigate the influence of roughness on samples with different crystalline orientation, we have grown (100) Fe/Cr on MgO(100) substrates by sputter deposition at different pressures (4, 7, and 11 mTorr) [see Fig. 3(a) for their low-angle XRD spectra]. Unlike in the (110) samples,[4] no drastic changes are observed in the LAXRD. The finite size peaks (in between the Bragg superlattice peaks) are clearly visible for the 11 mTorr sample, and the Bragg peaks remain sharp unlike in the (110) samples.[4] The immediate conclusion is that an increased sputtering pressure does not disorder the interfaces of (100) Fe/Cr samples to the same degree as it does on (110) samples. The mechanism by which this happens is not clear at this time, however for the purposes of this work it only matters that there is a controllable growth parameter which changes the structure in a reproducible way. The only structural effect we noticed in (100) with high pressures is an increase of the high-angle rocking curve width for the 11 mTorr samples. FWHM's of 4 and 7 mTorr samples are typically 1.5°–3°, whereas in the 11 mTorr samples it is 3°–5°. It thus seems that the increased deposition pressure disorders the bulk structure of (100) samples rather than the interfaces.

The transverse spin-dependent magnetoresistance at liquid helium temperatures is plotted in Fig. 3(c) as a function
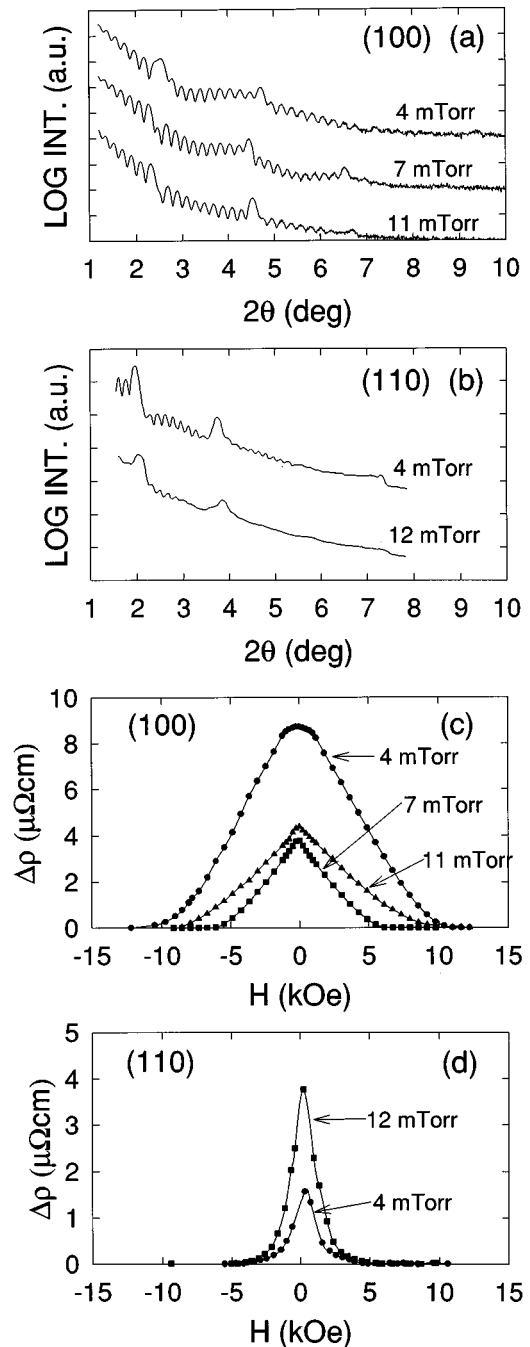

FIG. 3. Log plot of the low-angle x-ray diffraction scans for (100) samples (a) and (110) samples (b) at different sputtering pressures. These curves are offset for clarity. Spin-dependent magnetoresistance as a function of in-plane transverse magnetic field for the (100) samples grown at different pressures and the same Cr thickness (~15 Å) (c), and for sputtered (110) samples (d).

of the applied magnetic fields. In this case the dependence of $\Delta\rho$ is *nonmonotonic* with sputter pressures which is different from observations on the (110) samples. Although we have not made a systematic study of such effect as a function of Cr thickness, we did grow samples with Cr thicknesses around the optimum ~15 Å and found the same behavior. Due to the fact that the 11 mTorr samples have an overall greater resistivity than the 4 and 7 mTorr samples (Fig. 1), the magnetoresistance ratio $\Delta\rho/\rho$ steadily decreases over all
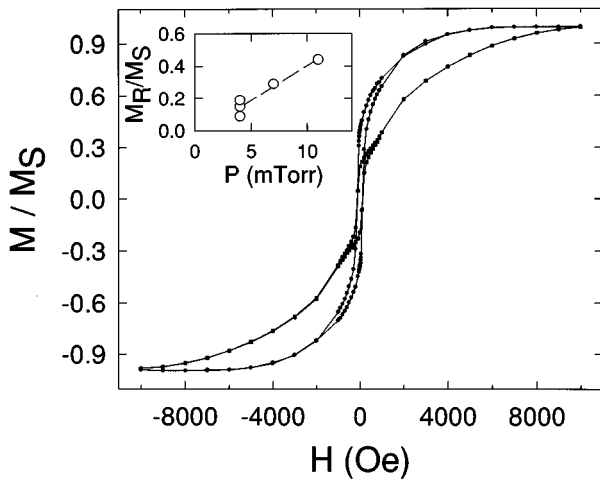
FIG. 4. Magnetization curves at 10 K for two samples with the same Cr thickness (15 Å) and different deposition pressures: (●) 4 mTorr and (■) 11 mTorr. The applied magnetic field is in the film plane and parallel to a substrate {100} direction. The inset shows the remanence to saturation ratio for samples grown at different pressures and Cr=15 Å. The three points at 4 mTorr are from samples that came out with different rocking curve widths (1.9°–3.7°).

the deposition pressure range tested. These results can tentatively be explained by a damage of the bulk crystallinity with increased sputter pressures, although the 7 mTorr samples do not exhibit a clearly broader rocking curve width than the 4 mTorr samples but do have a smaller $\Delta\rho$.

This is in agreement with the magnetization hysteresis loops. 11 mTorr (100) samples have a remarkably larger remanent magnetization than 4 mTorr samples as it shows in Fig. 4. More specifically, the inset shows that the ratio of the remanent magnetization to the saturation magnetization, M_R/M_S, i.e., a measure of the ferro coupling, increases with sputter pressure; from 0.1–0.2 (4 mTorr) to ~0.45 (11 mTorr), indicating a loss of antiferromagnetic coupling. Moreover, measurements on three 4 mTorr samples showed no dependence of M_R/M_S on the rocking curve width.

Therefore the decrease in the GMR can at least in part be assigned to this observed loss in AF coupling. The low squareness of these hysteresis loops can be related to the in-plane crystallografic and magnetic structure. From in-plane x-ray scans, we know that in our samples the Fe/Cr {100} directions are aligned to {110} MgO axis in a fourfold symmetry. Therefore, some shearing of the magnetization probably arises from the 45° deviation of the Fe/Cr {100} easy axis with the measuring magnetic field direction ({100} MgO). At this point, we have not found any further correlation of in-plane crystalline structure with magnetotransport properties.

CONCLUSIONS

In closing, we have found that growth optimization and low saturation resistivities are desirable to obtain very large values of GMR ($\Delta\rho/\rho$). Mosaicity plays an important role in the saturation resistivity of (100) samples with rocking curve width ($\Delta\varphi$), whereas is constant in (110) samples. The spin-dependent magnetoresistance values ($\Delta\rho$) of MBE and sputtered samples can be comparable, but its dependence on the structural parameters is quite different. Increasing the sputtering pressure of (100) Fe/Cr samples does not disorder the interface structure as it does in (110) sputtered multilayers. Rather, it increases the mosaic spread of the crystallites and, as a consequence, the magnetoresistance changes nonmonotonically with pressures.

*Present address: Research Institute for Materials, K. U. Nijmegen, The Netherlands.

†Present address: Materials Science Division, Argonne National Labs., Argonne, IL 60439.

‡Present address: Philips Research Laboratories, Eindhoven, The Netherlands.

[1] M. N. Baibich, J. M. Broto, A. Fert, F. Nguyen Van Dau, F. Petroff, P. Etienne, G. Creuzet, A. Friederich, and J. Chazelas, Phys. Rev. Lett. **61**, 2472 (1988).

[2] P. Grünberg, R. Schreiber, Y. Pang, M. B. Brodsky, and H. Sowers, Phys. Rev. Lett. **57**, 2442 (1986).

[3] S. S. Parkin, N. More, and K. P. Roche, Phys. Rev. Lett. **64**, 2304 (1990).

[4] E. E. Fullerton, D. M. Kelly, J. Guimpel, I. K. Schuller, and Y. Bruynseraede, Phys. Rev. Lett. **68**, 859 (1992).

[5] R. Schad, C. D. Potter, P. Beliën, G. Verbanck, V. V. Moshchalkov, and Y. Bruynseraede, Appl. Phys. Lett. **64**, 3500 (1994).

[6] E. E. Fullerton, M. J. Conover, J. E. Mattson, C. H. Sower, and S. D. Bader, Appl. Phys. Lett. **63**, 1699 (1993).

[7] C. D. Potter, R. Schad, P. Beliën, G. Verbanck, V. V. Moshchalkov and Y. Bruynseraede, Phys. Rev. B **49**, 16 055 (1994).

[8] A. R. Modak, D. J. Smith, and S. S. P. Parkin, Phys. Rev. B **50**, 4232 (1994).

[9] F. Petroff, A. Barthelémy, A. Hamzic, A. Fert, P. Etienne, S. Lequien, and G. Creuzet, J. Magn. Magn. Mater. **93**, 95 (1991).

[10] S. S. P. Parkin, T. A. Rabedeau, and A. Modak (unpublished).

[11] E. E. Fullerton, M. J. Conover, J. E. Mattson, C. H. Sowers, and S. D. Bader, Phys. Rev. B **48**, 15 755 (1993).

[12] N. M. Rensing, A. P. Payne, and B. M. Clemens, J. Magn. Magn. Mater. **121**, 436 (1993).

[13] E. E. Fullerton, I. K. Schuller, and Y. Bruynseraede. Mater. Res. Soc. Bull. **16**, 33 (1992).

[14] E. E. Fullerton, I. K. Schuller, H. Vanderstraeten, and Y. Bruynseraede, Phys. Rev. B **45**, 9292 (1992).